the case for the two cyclic forms with the carbon-carbon double bond endo (**4C** and **5D**), in which the cyclohexene ring probably assumes a half-chair conformation with the C6-C1-C2-C3 moiety planar.[45] On the other hand, the cyclic forms with exo orientation of the double bond (**4D** and **5C**) prefers a chair conformation of the six-membered rings with a considerable torsional angle about the C1-C2 bond.[46] Increasing this torsional angle from zero weakens the hydrogen bond and may cause the observed shifts in the binding energies.

Conclusions

1. The XPS technique shows that for β-thioxoketones both the O_{1s} and S_{2p} regions exhibit ionizations from the enol (**2D**) as well as the enethiol (**2C**) form, thereby confirming that β-thioxoketones exist as rapidly interconverting enol and enethiol tautomers.

2. The position of the tautomeric enol-enethiol equilibrium has been determined by XPS based on the relative areas of the peaks in the O_{1s} ionization regions. The S_{2p} region seems to be less suitable for quantitative determinations due to the presence of sulfur spin-orbit splitting but confirms nevertheless the conclusions derived from the O_{1s} region. This represents a limitation of the XPS technique for determining positions of tautomeric equilibria in systems having heteroatoms giving rise to spin-orbit splitting. However, fortunately for these systems, the presence of oxygen yields satisfactory results.

3. The nonexistence of the thioxoketone form **2A** has been further confirmed for thioacetylacetone (**3**).

4. The binding energies of the compounds studied (Figure 6) suggest that geometrical constraints in the cyclic β-thioxoketones **4** and **5** may be reflected in the strength of the intramolecular hydrogen bond.

The above conclusions confirm that X-ray photoelectron spectroscopy is suitable for qualitative as well as quantitative studies of tautomeric equilibria in the gas phase, here exemplified by the enol-enethiol equilibrium in the β-thioxoketones.

Acknowledgment. We are grateful to the National Research Council of Canada and to the Danish Natural Science Research Council for financial support.

Registry No. 3, 14660-20-9; **4**, 76698-82-3; **5**, 15578-82-2; **6**, 78429-69-3; **7**, 40553-10-4.

(45) J. Dale, "Stereokjemi og Konformasjonsanalyse", Scandinavian University Books, Oslo, 1975.

(46) The torsional angle between the exocyclic double bonds in 1,2-dimethylencyclohexane amounts to about 60°; see P. Asmus and M. Klessinger, *Tetrahedron*, **30**, 2477 (1974).

Phase-Transition Behavior of Saturated, Symmetric Chain Phospholipid Bilayer Dispersions Determined by Raman Spectroscopy: Correlation between Spectral and Thermodynamic Parameters

Ching-hsien Huang,*[1] Jeffrey R. Lapides, and Ira W. Levin*

Contribution from the Laboratory of Chemical Physics, National Institute of Arthritis, Diabetes, and Digestive and Kidney Diseases, National Institutes of Health, Bethesda, Maryland 20205.
Received February 16, 1982

Abstract: The phase-transition characteristics for the members of an homologous series of saturated, symmetrical phosphatidylcholine bilayer dispersions were investigated by Raman spectroscopy for the even carbon chain length systems extending from C(10) to C(22). Peak-height intensity ratios involving vibrational transitions in the 3000-cm^{-1} acyl chain methylene carbon-hydrogen (C-H) stretching mode region were used to construct temperature profiles reflecting phospholipid order/disorder processes. Although temperature profiles derived from the C-H stretching mode spectral parameters emphasize the gel to liquid crystalline phase transition at T_m, while generally deemphasizing the pretransition bilayer reorganizations in comparison to profiles based upon C-C stretching mode ratios, two-phase transitions are clearly discerned for diC(12)PC. The lower transition exhibits a sensitivity to the thermal history of the sample in contrast to an invariance in the behavior of the higher temperature order/disorder process at 3.3 °C, which we attribute to the primary gel to liquid crystalline phase transition. For diC(10)PC the temperature profile displays a phase transition at −8.5 °C which is associated with the order/disorder process for the system reorganizing from an immobile lamellar phase to possibly a dynamic micellar phase. The temperature profile derived from the Raman spectral parameters for 1-C(16)lysoPC, a system known to form micelles at room temperature, exhibits a sharp phase transition at 5.2 °C, which is also attributed to a transition between the lamellar and micellar phases. For the systems undergoing bilayer gel to liquid crystalline phase transitions, the parameter ΔI_R, which represents changes in the Raman intensity ratio across T_m, is correlated with ΔS, the entropy change determined at T_m for these phospholipids by calorimetric measurements.

Raman spectroscopy has been widely employed in recent years in investigating the lipid conformation and dynamics in both model and biological membranes.[2] The advantage of this technique over many other physical methods lies in the sensitivity of the vibrational spectra of lipid assemblies to bilayer reorganizations and to the changes in population of various bond conformations (gauche/trans ratios). Aqueous dispersions of synthetic phospholipids in bilayers undergo a highly cooperative endothermic phase transition from the gel to the liquid crystalline state when they are heated above a characteristic phase-transition temperature, T_m.[3] Thermodynamically, this phase transition is characterized by a marked increase in entropy; conformationally, it is described by an abrupt increase in intramolecular acyl chain disorder accompanied by a simultaneous decrease in chain-chain

(1) On sabbatical leave from the Department of Biochemistry, University of Virginia School of Medicine, Charlottesville, Virginia 22908.

(2) For a recent review, see: Lord, R. C.; Mendelsohn, R. In "Membrane Spectroscopy"; Springer-Verlag: New York, 1981; pp 337-426.

(3) Phillips, M. C.; Williams, R. M.; Chapman, D. *Chem. Phys. Lipids* **1969**, *38* 134-244.

contact interactions. The application of Raman spectroscopy in studying the bilayer gel → liquid crystalline phase transition is particularly revealing, since the phase-transition behavior is monitored by temperature-dependent changes in the frequencies and intensities of appropriate vibrational modes which reflect alterations within either the head-group, interface, or acyl chain region of the membrane.

Although the phase transitions of a large number of synthetic phospholipid dispersions have been measured by differential scanning calorimetry, only a limited number of symmetric phosphatidylcholines have been systematically investigated by Raman spectroscopy. In this paper we examine, as a function of temperature, the Raman spectral changes in the hydrocarbon chain C–H stretching mode regions of an homologous series of saturated, symmetric chain phosphatidylcholines. Our results suggest that the intensity alterations observed in the vibrational spectra are correlated with the thermodynamic parameters determined by calorimetry as multilamellar dispersions undergo their gel to liquid crystalline phase transitions. In addition, our studies reveal, for the first time, the thermotropic behavior of the short-chain, diacyl phospholipid dispersions, diC(12)PC and diC(10)PC.[4]

Experimental Section

All synthetic saturated phosphatidylcholines were obtained from Avanti Polar Lipids, Inc., Birmingham, AL., except for diC(14)PC, diC(18)PC and 1-palmitoyllysoPC, which were purchased from Calbiochem-Behring Co., San Diego, CA. Prior to use, the commercial lipids, claimed to be 99% pure, were dissolved in cyclohexane and then precipitated with acetone. After drying, the white precipitates were dispersed in a minimum volume of distilled water at a temperature 5–10 °C above the main transition temperature (T_m) of the phospholipid. This liquid dispersion was frozen by liquid N_2 and lyophilized overnight. The lyophilized sample (6–10 mg) was mixed with 12–20 μL of 75 mM NaCl. This lipid suspension (33.3% lipid in 50 mM NaCl, w/w) was kept at a temperature 5–10 °C above T_m for 30 min. A 10–20-μL sample was injected into a Kimax glass capillary (i.d. 1.25 mm) and then spun in a bench-top clinical centrifuge. After the sample capillary was sealed, the tube was inserted into a thermostatically controlled sample holder and optically aligned within the Raman spectrometer. While in place the sample was first cooled to a temperature 10–15° below T_m at a cooling rate of approximately 25° h^{-1} and then equilibrated in the laser beam at this temperature for at least an additional 30 min before recording spectral scans. All solvents and reagents used were either ultrapure or spectral grade. The purity of the lyophilized phospholipid was ascerted by thin-layer chromatography (TLC) with the solvent mixture chloroform/methanol/48% ammonium hydroxide (65/35/5). After acetone precipitation, hydration, and lyophilization, all synthetic phospholipids were judged pure by TLC techniques since only a single spot was detected with iodine after migration in the developing solvent of 1–2 μmol of the lipid sample.

Vibrational Raman spectra were recorded with a Spex Ramalog 6 spectrometer equipped with holographic gratings. A Coherent Radiation Model CR-12 argon ion laser, delivering 200 mW of power at the sample at 514.5 nm, served as the excitation source. Since the 2800–3100-cm^{-1} C–H stretching mode region involves relatively broad spectral features, a spectral resolution of ~5 cm^{-1} was satisfactory for monitoring bilayer phase-transition characteristics. Spectral frequencies, calibrated with atomic argon and laser plasma lines, are reported to ±2 cm^{-1}. Sample temperatures, reported to ±0.1 °C, were monitored by a copper–constantan thermocouple placed adjacent to the sample capillary within the thermostatically controlled assembly. Heating curves proceeded from low to high temperature in obtaining temperature profiles of the bilayer dispersions. Samples were equilibrated between temperatures for 7.5 min for the diC(12)PC system and 10 min between temperatures for all other systems prior to acquiring Raman spectra with a Nicolet NIC-1180 data system interfaced to the spectrometer. Signal averaging techniques, requiring 3–4 scans per temperature interval, yielded satisfactory spectra for spectral intensity ratio determinations. No computer smoothing routines were involved in the data reduction. The temperature interval for the diC(12)PC system was 1 °C, while the intervals for the other systems were 2 °C. Temperature profiles were constructed from peak-height intensities for the I_{2936}/I_{2885} interchain order/disorder parameters. The temperature profiles derived from the C–H stretching region parameters, shown in Figure 2 for the series from diC(14)PC to diC(18)PC, deemphasize the pretransition phenomenon, in contrast to the profiles derived from the C–C stretching region data (plots not shown). For the diC(20)PC and diC(22)PC multilamellar dispersions, the pretransitions occur too close to the main transition to be detected by the Raman technique.

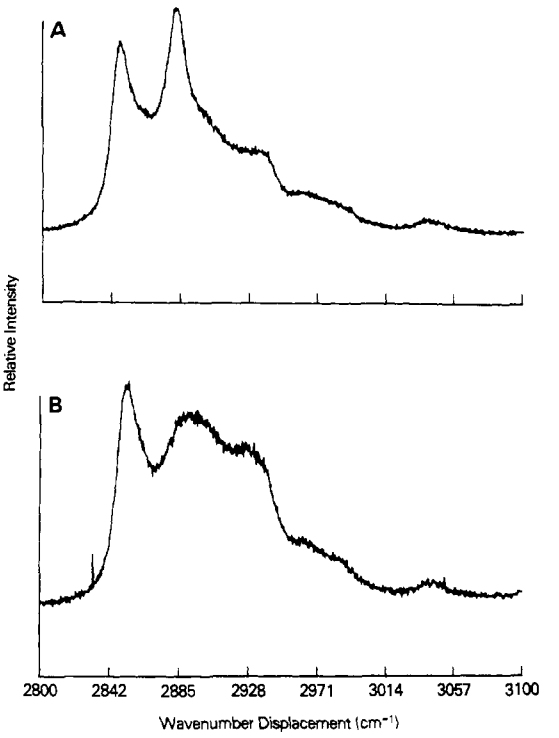

Figure 1. Raman spectra of diC(20)PC in the 2900-cm^{-1} hydrocarbon C–H stretching mode region for (A) the gel state at 51.4 °C and (B) the liquid crystalline state at 75.4 °C.

Results and Discussion

Since the methylene C–H stretching mode region provides the most intense spectral features in the Raman spectrum of a lipid sample, the 2800–3100-cm^{-1} interval has been commonly used to monitor changes in the lipid chain lateral packing properties in both gel and liquid crystalline uni- and multilamellar bilayer systems.[5,6] Figure 1 presents representative Raman spectra in the C–H stretching mode region of diC(20)PC dispersions in the gel (Figure 1A) and liquid crystalline (Figure 1B) states. Although the vibrational assignments have been discussed previously,[5,7-9] we briefly summarize here the observed spectral features. As shown in Figure 1A, the spectrum of the gel state at 51.4 °C, the methylene C–H symmetric and asymmetric stretching modes appear as intense, partially overlapped features at 2847 and 2883 cm^{-1}, respectively. The 2936-cm^{-1} peak represents, in part, a Fermi resonance component of the acyl chain terminal methyl C–H symmetric stretching mode.[10] During the bilayer intramolecular chain-disordering process, which occurs on heating the dispersions, the intensity in the 2936-cm^{-1} region increases, while the peak broadens, as an underlying manifold of infrared-active methylene C–H asymmetric stretching modes are rendered active in the

(4) Abbreviations used: diC(10)PC, β,γ-dicapryl-L-α-phosphatidylcholine; diC(12)PC, β,γ-dilauryl-L-α-phosphatidylcholine; diC(14)PC, β,γ-dimyristoyl-L-α-phosphatidylcholine; diC(16)PC, β,γ-dipalmitoyl-L-α-phosphatidylcholine; diC(18)PC, β,γ-distearoyl-L-α-phosphatidylcholine; diC(20)PC, β,γ-diarachidoyl-L-α-phosphatidylcholine; diC(22)PC, β,γ-dibehenoyl-L-α-phosphatidylcholine; lysoPC, L-α-lysophosphatidylcholine; 1-C(16)lysoPC, 1-palmitoyllysophosphatidylcholine; TLC, thin-layer chromatography. The conventional use of C(x), where x is position number, in being modified. In this paper x is defined as carbon chain length.

(5) Yellin, N.; Levin, I. W. *Biochim. Biophys. Acta* **1977**, *489*, 177–190.
(6) Synder, R. G.; Scherer, J. R.; Gaber, B. P.; *Biochim. Biophys. Acta* **1980**, *601*, 47–53.
(7) Gaber, B. D.; Peticolas, W. L. *Biochim. Biophys. Acta* **1977**, *465*, 260–274.
(8) Spiker, R. C.; Levin, I. W. *Biochim. Biophys. Acta* **1976**, *455*, 560–575.
(9) Bunow, M.; Levin, I. W. *Biochim. Biophys. Acta* **1977**, *487*, 388–394.
(10) Hill, I. R.; Levin, I. W. *J. Chem. Phys.* **1979**, *70*, 842–851.

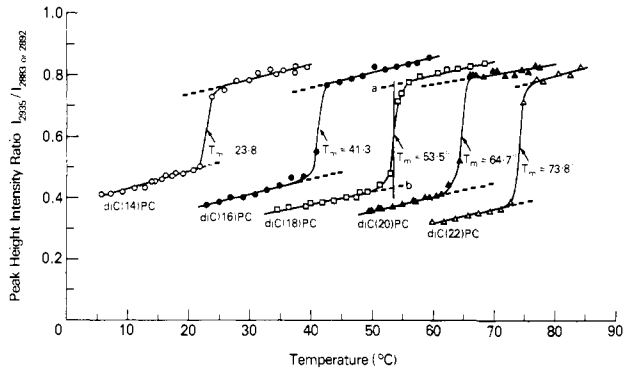

Figure 2. Temperature profiles for a series of saturated, symmetric phosphotidylcholines with the Raman spectral $I_{2936}/I_{2883(or2892)}$ peak-height intensity ratios as indices.

Raman effect.[9] In contrast, the 2883-cm^{-1} feature decreases in intensity and shifts in frequency to 2892 cm^{-1} (Figure 1B) as the bilayer disorders and enters the liquid crystalline state at 75.4 °C. It is evident in Figure 1A that below T_m the narrow, intense 2883-cm^{-1} peak is superimposed upon a relatively broad background band, which essentially disappears above T_m, as indicated by Figure 1B. This background has been assumed to arise from a Fermi resonance interaction between the symmetric methylene C–H stretching fundamental at 2847 cm^{-1} and the continuum of binary combinations of the methylene bending fundamentals of the extended hydrocarbon chain.[11,12] In the liquid crystalline state the half-width of the 2883-cm^{-1} line increases several fold. Further, the Fermi resonance interaction with the 2847-cm^{-1} line is now removed as a consequence of vibrational decoupling induced by the introduction of gauche conformers along the chain.[11] Since the empirical $I_{2936}/I_{2883(2892)}$ peak-height intensity ratio has been demonstrated to be a measure of the interchain order/disorder processes of the lipid acyl chains in bilayers,[5] we use this spectral parameter to compare the members of the present series of phospholipid dispersions. We emphasize that although the C–H stretching mode region consists of a congested, complex set of vibrational transitions, the peak-height intensity ratios described above provide an extraordinarily sensitive probe for monitoring intramolecular (conformational) chain disorder concomitantly with intermolecular chain–chain packing disorder. Thus, the Raman technique is particularly useful in discerning the highly cooperative phase-transition characteristics of the bilayer as the system passes from the gel to the liquid crystalline state.

For completeness, we note in Figure 1A that the features at ~2956 and ~2960 cm^{-1} are assigned to the acyl chain terminal methyl asymmetric stretching modes and a superposition of the choline methyl symmetric C–H stretching modes at ~2986 cm^{-1}.[13] The weak, symmetrical peak at 3042 cm^{-1} is assigned to the choline methyl asymmetric C–H stretching fundamentals.[13]

Figure 2 presents the changes in the Raman peak-height intensity ratio as a function of temperature for an homologous series of saturated symmetric like-chain PCs in the form of multilamellar bilayer dispersions in excess 50 mM NaCl solutions. In no case were the errors in the Raman peak-height intensity ratio greater than ~3%. All lipids show an abrupt increase in the spectral ratio at their characteristic phase-transition temperatures. As shown in the temperature profiles for diC(18)PC given in Figure 2, the linear portions of the profile above and below the phase transition are extended by a linear least-squares fit. The main phase-transition temperature T_m is operationally defined as the midpoint temperature at which the Raman intensity ratio equals $^1/_2(a + b)$, where a and b are, respectively, the Raman intensity ratios at a given temperature in the extended linear portions of the upper and lower ends of the transition curve. In these curves, the Raman intensity ratio of I_{2936}/I_{2883} is used for the temperature region below T_m, while I_{2936}/I_{2892} is used to calculate the Raman intensity ratio at temperatures above T_m as a consequence of the frequency shift for the methylene C–H asymmetric stretching modes above T_m. The transition temperatures are 73.8, 64.7, 53.5, 41.3, and 23.8 °C, respectively, for lipid dispersions of diC(22)PC, diC(20)PC, diC(18)PC, diC(16)PC, and diC(14)PC. These values are in excellent agreement with calorimetric data, as summarized in Table I.

Table I. Summary of the Order/Disorder Transition Data of Phospholipid Dispersions Derived from Raman Spectral Parameters

dispersions	T_m,[a] °C	ΔI_R at T_m	$\Delta I_R{}^{eff}$	T_m,[b] °C	ΔS,[b] (eu/mol)
diC(10)PC	−8.5	0.232			
diC(12)PC	−4.3, 3.3	0.127, 0.129		−1.8	6.27
diC(14)PC	23.8	0.252	0.111	24	18.2
diC(16)PC	41.3	0.299	0.158	41	27.4
diC(18)PC	53.5	0.340	0.199	55	32.3
diC(20)PC	64.7	0.368	0.227		
diC(22)PC	73.8	0.395	0.254	75	42.5

[a] Transition temperatures determined by peak-height intensity ratios derived from the hydrocarbon CH stretching region (see Figure 2). [b] Thermodynamic parameters taken from ref 15. These data are derived from calorimetric data of ref 3, 14, and 20.

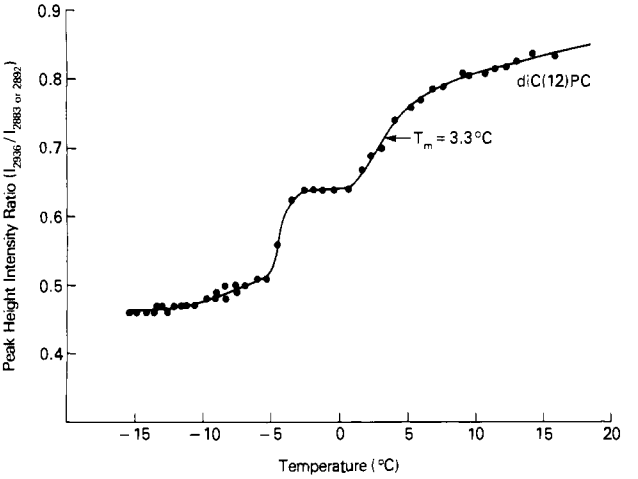

Figure 3. Temperature profile for diC(12)PC showing two order/disorder transitions in the −15 to 16 °C temperature range.

The behavior of the peak-height intensity ratio of diC(12)PC dispersions, as a function of temperature ranging from −15 to 16 °C, shows two clearly discernible phase transitions (Figure 3). The lower temperature transition appears to be sharper than the upper one. A similar result was reported for this short-chain phospholipid dispersion by Mabrey and Sturtevant[14] using high-sensitivity differential scanning calorimetry. In marked contrast to the higher temperature transition, the lower one is extremely sensitive to the thermal history of the sample; both the magnitude of the Raman spectral ratio and the transition temperature can be shifted, depending on the pretreatment of the sample. If the diC(12)PC dispersions were first kept at a temperature near the higher transition temperature (3.3 °C) for 24 h, incubated for an hour in the sample holder at −15 °C, and then scanned, the Raman intensity ratio profile displays a broad single transition with an onset temperature of −3.5 °C at a Raman intensity ratio of 0.42. In contrast, if the sample was kept at −7 °C, which is below the lower transition temperature (−4.3 °C), for 24 h and then scanned from −15 °C, the onset temperature of this rather broad single transition is −7.5 °C; under these conditions the Raman intensity ratio at the base line is 0.52. That is, the gel state is now more disordered and the lower order/disorder phase

(11) Synder, R. G.; Hsu, S. L.; Krimm, S. *Spectrochim. Acta, Part A* **1978**, *34A*, 395–406.
(12) Snyder, R. G.; Scherer, J. R. *J. Chem. Phys.* **1979**, *71*, 3221–3228.
(13) Spiker, R. C.; Levin, I. W. *Biochim. Biophys. Acta* **1975**, *388*, 361–373.
(14) Mabrey, S.; Sturtevant, J. M. *Proc. Natl. Acad. Sci. U.S.A.* **1976**, *73*, 3862–3866.

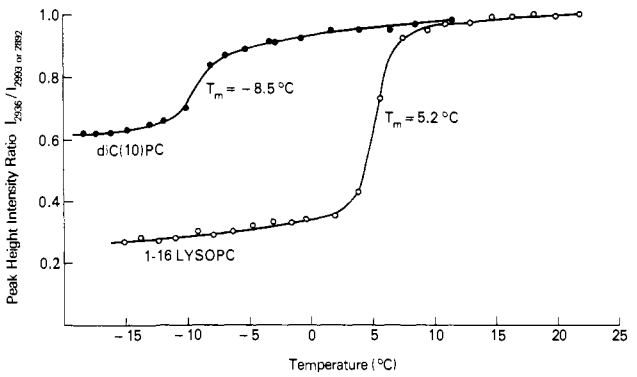

Figure 4. Comparison of the temperature profiles for diC(10)PC and 1-C(16)lysoPC with the $I_{2936}/I_{2883(or2892)}$ peak-height intensity ratios as markers.

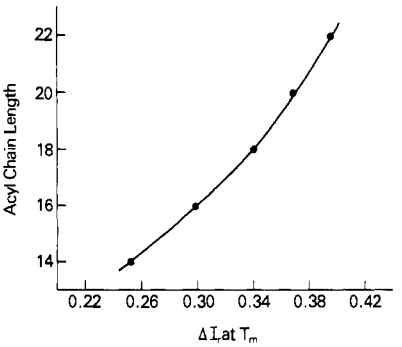

Figure 5. Behavior of ΔI_R, the change in the Raman peak-height intensity ratios (for the C–H stretching mode region) across the main-phase transition region at T_m, as a function of the acyl chain length for various saturated phospholipids.

transition occurs at a lower temperature. In both cases, however, the transition profiles in the region of 1.5–16.0 °C are virtually indistinguishable from the one shown in Figure 3.

A 33.3% diC(12)PC dispersion in 99.9% D_2O was investigated by Raman spectroscopy in order to demonstrate that the two-transition profile of diC(12)PC dispersions observed in Figure 3 is an inherent lipid property and not caused by the ionic environment or the density of the suspending medium. If the sample was annealed and slowly cooled to −15 °C in the sample holder prior to recording the spectra, a two-transition profile of the diC(12)PC–D_2O sample was also observed (data not shown). Again, the lower temperature transition is sensitive to the pretreatment of the sample. Since the higher transition is insensitive to the thermal history, a behavior exhibited by all other longer diacyl symmetric-chain phospholipid dispersions for their main-phase transitions, we consider the higher temperature transition to be the main transition of diC(12)PC dispersions, in contrast to the conclusion of ref 14.

Figure 4 presents the plot of the peak-height Raman spectral intensity ratio as a function of temperature for diC(10)PC dispersions. It is recognized that a phase transition with a T_m of −8.5 °C does indeed occur within the temperature range studied. This result is totally unexpected because thermodynamic parameters, such as the change in enthalpy (ΔH), entropy (ΔS), and partial molar volume (ΔV), associated with the phase transition of multilamellar bilayer dispersions of diC(10)PC can be calculated to be close to zero.[15] It should be noted, however, that our earlier thermodynamic prediction was based on calorimetric data associated with the gel → liquid crystalline phase transition in various lamellar phospholipid dispersions. If, in excess water, diC(10)PC forms structural assemblies in which the lamellar arrangement is no longer retained, then our thermodynamic prediction cannot be applied to this short-chain, synthetic phospholipid. In fact, the values of the spectral ratio of diC(10)PC dispersions in the linear part of the temperature profile above T_m (Figure 4) are considerably higher than any of the corresponding values obtained with other diacyl phospholipid dispersions (Figures 2 and 3), indicating that the lipid acyl chains in this system at temperatures above T_m are more disordered conformationally than other longer acyl chains in multilamellar diacyl phospholipid bilayers at an equivalent temperature relative to T_m. One reasonable interpretation is that, at temperatures above T_m (−8.5 °C), diC(10)PCs in excess water form micelles instead of bilayers, and the observed transition in Figure 4 is associated with an order/disorder process in which the lipid molecules reorganize from a relatively immobile lamellar phase to a dynamic, micellar phase.

In order to demonstrate that diC(10)PC forms micelles in excess water at temperatures above T_m, we have compared our Raman results with those obtained from 1-palmitoyllysoPC. LysoPCs are well-known to form micelles in excess water at room temperature.[16] Figure 4 displays the Raman intensity ratios, as a function of temperature, of 1-palmitoyllysoPC and diC(10)PC dispersions (33% w/w). Our results clearly indicate that the lysoPC dispersions displays a sharp thermotropic transition at 5.2 °C. Recently, Van Echteld et al.[17] also reported a similar transition associated with the lamellar → micellar reorganization of 1-palmitoyllysoPC dispersions using ^{31}P NMR spectroscopy and freeze-fracture electron microscopy. The nearly identical values for the Raman spectral ratios for diC(10)PC and 1-palmitoyllysoPC dispersions at temperatures above T_m suggest that diC(10)PC forms micelles in excess water above T_m. We should also point out that the Raman intensity ratios for diC(10)PC and 1-palmitoyllysoPC are quite different at temperatures below T_m, suggesting that the lipid molecules are packed differently in the lamellar phase for the two systems. It is quite possible that diC(10)PC dispersions, similar to diC(12)PCs, may display a two-transition profile. Our current cooling capacity is limited in achieving temperatures below −20 °C; hence, any additional spectral ratio change that may occur below −20 °C cannot easily be detected by our instrumentation.

It is interesting to point out that the Raman peak-height intensity ratios, I_{2936}/I_{2892}, measured at temperatures higher than T_m for various saturated like-chain phosphatidylcholines in the multilamellar bilayer structure, differ from one another by only a small fraction with the value increasing with increasing chain length (Figure 2). For instance, the values of I_{2936}/I_{2892} (%) measured at 10 °C higher than T_m for diC(20)PC, diC(18)PC, diC(16)PC, and diC(14)PC are 82.3, 82.1, 81.8, and 80.6, respectively. Thus, the longer chain systems show a trend to greater disorder in the liquid crystalline state. In contrast, the intensity ratio, I_{2936}/I_{2883}, measured at temperatures below T_m decreases with increasing chain length (Figure 2). At a temperature 10 °C below T_m, for instance, the values of I_{2936}/I_{2883} (%) are 33.2 37.7, 39.0, 41.7, and 45.0 for diC(22)PC, diC(20)PC, diC(18)PC, diC(16)PC, and diC(14)PC, respectively. That is, in the gel state the long-chain systems exhibit a more ordered packing configuration. It is evident from Figure 3 that diC(12)PC dispersions display an anomalous transition profile; its intensity ratios do not follow the general pattern exhibited by other longer phospholipid dispersions discussed above. Clearly, further work is needed to characterize this system. Because of the anomaly, it is doubtful that diC(12)PC dispersions at temperatures above upper T_m adopt only a large multilamellar bilayer structure; consequently, we will not include this system in correlating the properties of typical large multilamellar bilayers in excess water.

The difference ΔI_R in the Raman intensity ratio across the main phase-transition region at T_m is plotted as a function of the acyl chain length for various lamellar phospholipids in Figure 5. The plot demonstrates that the spectroscopic changes in the Raman region of 2800–3100 cm^{-1} accompanying the gel → liquid crystalline phase transition follow a curvilinear, rather than a linear, behavior as a function of the acyl chain length. Analogously, the

(15) Mason, J. T.; Huang, C. *Lipids* **1981**, *16*, 604–608.
(16) Reiss-Husson, F. *J. Mol. Biol.* **1967**, *25*, 363–382.
(17) Van Echteld, C. J. A.; DeKruijff, B.; Mandersloot, J. G.; DeGier, J. *Biochim. Biophys. Acta* **1981**, *649*, 211–220.

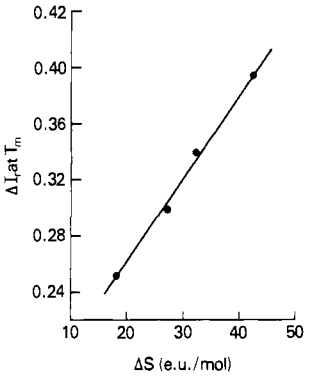

Figure 6. Linear correlation between ΔI_R and the transition entropy ΔS for the homologous series of saturated phospholipids diC(14)PC, diC(16)PC, diC(18)PC, and diC(22)PC. (See text and the caption for Figure 5 for the definition of ΔI_R.)

thermodynamic parameters of the phospholipid phase transition, such as ΔS, ΔH, and ΔV, also increase with increasing acyl chain length in a curvilinear fashion.[15]

The differences in the Raman intensity ratios ΔI_R at T_m are plotted in Figure 6 against the calorimetrically determined gel to liquid crystalline phase-transition entropy changes (ΔS) for the various multilamellar phospholipid dispersions. For this plot the linear regression fit yields a slope of 0.0060 ± 0.0003 (with a correlation coefficient of 0.9968) and an intercept on the ΔI_R axis of 0.141 ± 0.004. The finite value for ΔI_R as the transition entropy (ΔS) is extrapolated to zero suggests that the entropy change at the phase transition contains a negative term and that the order/disorder process associated with this specific contribution cannot be monitored by the Raman spectral ratios recorded in the 2900-cm^{-1} region. A physical basis for negative entropy contributions at the phase transition lies in the change in the degree of hydration of the bilayers. Using ^1H NMR techniques, Taylor et al.[18] have shown that the hydration of synthetic phospholipid dispersions increases significantly when the systems are heated from the gel to the liquid crystalline state. A similar conclusion on the effect of the gel → liquid crystalline phase transition on phospholipid hydration was drawn by Watts et al.[19] using hydrodynamic techniques. The interpretation of these observations is very simple. As the phospholipid bilayer undergoes an endothermic phase transition, the bilayer surface expands; consequently, more water molecules partition into the bilayer and interact with the polar head group. From these studies it is evident that the entropy contribution from the water molecules interacting with the polar head group must be negative at the phase transition. Since the Raman peak height intensity ratio differences derived from the C–H stretching mode region do not detect the order/disorder transition of water molecules associated with the phase transition, a plot of ΔI_R at T_m against ΔS should yield a positive intercept on the ΔI_R axis.

The linear relationship between the Raman spectroscopic changes and the transition entropy changes accompanying the phase transition for various lamellar phospholipids, as shown in Figure 6, is an intriguing observation and deserves further discussion. The transition entropy (ΔS) is a measure of the total entropy change of the phospholipid bilayer, in excess water, from the gel to the liquid crystalline states at the transition temperature; it equals the transition enthalpy change (ΔH) divided by T_m, or $\Delta S = \Delta H/T_m$. The magnitude of the transition entropy, calculated from calorimetric data, can be considered, to a first approximation, as the sum of intrachain configurational entropy (ΔS_1), the interchain disordering entropy (ΔS_2), and the entropy of the water molecules interacting with the polar head groups (ΔS_3) by the expression $\Delta S \simeq a_1\Delta S_1 + a_2\Delta S_2 + a_3\Delta S_3$, where a_n is the relative contribution of each specific entropy term (ΔS_n) to the overall transition entropy. From the temperature-dependent hydration studies of the synthetic phospholipid dispersions mentioned above, ΔS_3 must have a negative sign. ΔS_1 and ΔS_2, however, can be shown to be positive.[3] Since the Raman peak intensity ratio difference originating from the C–H stretching mode region reflects both the intrachain conformational order/disorder and the interchain contact order/disorder of the lipid acyl chains in the bilayer,[5] and since the spectral differences do not monitor the order/disorder transition of water molecules associated with the lipid phase transition, the change in ΔI_R for the various phospholipid dispersions across the phase transition is expected to correlate with either the sum of $a_1\Delta S_1$ and $a_2\Delta S_2$ or the difference between ΔS and $a_3\Delta S_3$ for the corresponding system. Our experimental results, reflected in Figure 6, support this conclusion. Although individual values for ΔS_n and a_n cannot be determined from the present data, the difference between the experimental value of ΔI_R at T_m from Figure 2 and the extrapolated value of the ΔI_R intercept (0.141) from Figure 6 defines an "effective" difference in Raman peak-height intensity ratios, ΔI_R^{eff}, at the transition temperature. This empirically derived ΔI_R^{eff} is then directly proportional to the transition entropy by the expression: $\Delta I_R^{eff} = (6 \times 10^{-3})\Delta S$. Values of ΔI_R^{eff} and ΔS associated with the gel → liquid crystalline phase transition of various multilamellar phospholipid dispersions are given in Table I.

In summary, we have performed Raman measurements to investigate the order/disorder transitions of various saturated phospholipid dispersions. The results are detailed in Table I. For comparison, the transition temperature and transition entropies of these systems calculated from calorimetric data are also included. A linear relationship between ΔI_R, the difference in the Raman peak-height intensity ratio across the order/disorder transition, and ΔS, the transition entropy across the lamellar gel → liquid crystalline phase transition, is clearly demonstrated. Moreover, the effective change in Raman peak-height intensity ratios, ΔI_R^{eff}, is directly proportional to ΔS through the expression $\Delta I_R^{eff} = (6 \times 10^{-3})\Delta S$. In addition, we show for the first time that diC(10)PC dispersions display an order/disorder transition that is attributed to the hydrocarbon conformational and packing changes associated with the phospholipids undergoing a reorganization from a lamellar bilayer to a micellar structure.

(18) Taylor, R. P.; Huang, C.; Broccoli, A. V.; Chun, J. K. *Arch. Biochem. Biophys.* **1978**, *187*, 197–200.
(19) Watt, S.; Marsh, D.; Knowles, P. F. *Biochemistry* **1978**, *17*, 1792–1801.
(20) Albon, N.; Sturtevant, J. M. *Proc. Natl. Acad. Sci. U.S.A.* **1978**, *75*, 2258–2260.

Registry No. diC(10)PC, 63700-87-8; diC(12)PC, 18194-25-7; diC(14)PC, 64234-00-0; diC(16)PC, 35418-55-4; diC(18)PC, 66701-63-1; diC(20)PC, 83061-18-1; diC(22)PC, 83061-19-2; 1-C(16)lysoPC, 14863-27-5.